ARCHIVE OF MECHANICAL ENGINEERING

DOI: 10.24425/ame.2022.144072 2023, Vol. 70, No. 1, pp. 63–83

Mehmet Ilteris SARIGECILI [1], Ibrahim Deniz AKCALI [1]

Modified Hooke-Jeeves optimization of operating parameters for required slider speeds and displacements in a feeder slider-crank mechanism

Received 31 December 2021, **Revised** 8 October 2022, **Accepted** 25 October 2022, **Published online** 5 December 2022

Keywords: slider-crank, dynamic model, speed control, Hooke-Jeeves method, optimization

In such applications as in the case of feeders in which a slider-crank mechanism equipped with a rotational spring on its crank is driven by a constant force and a lumped mass at the crank-connecting rod joint center, the slider is required to take on desired speeds and displacements. For this purpose, after obtaining and solving the dynamic model of the slider-crank mechanism, the output of this model is subjected to a modified Hooke-Jeeves method resulting in the development of a procedure for the optimization of selected set of operating parameters. The basic contribution involved in the so-called Hooke-Jeeves method is the procedure by which a cost-effective advancement towards a target optimum point is accomplished in a very short time. A user-friendly interface has also been constructed to support this procedure. The optimization procedure has been illustrated on a numerical example. The validation of the resulting dynamic model has also been demonstrated.

1. Introduction

Among many other applications, slider-crank mechanism utilized as a cutter and feeder in the design of a uniform ice cutting device is shown in Fig. 1 [1]. There are two distinct phases for the material removing process: (1) The cutter removes material from the raw material at a constant speed in its forward and backward motion once it contacts the raw material (i.e., contact phase). During the cutting process, the raw material is kept at rest by the feeder pushing it against the cutter under a constant pushing force. (2) In the no-contact phase, the cutter

✉ Mehmet Ilteris Sarigecili, e-mail: msarigecili@cu.edu.tr

[1]Department of Mechanical Engineering, Çukurova University, Adana, Turkey. ORCIDs: M.I.S. 0000-0002-9969-2005, I.D.A. 0000-0001-5194-5061

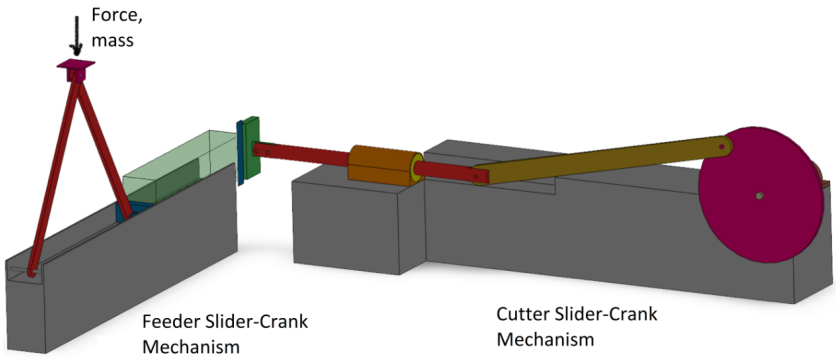

Fig. 1. Uniform ice cutting device [1]

moves forwards and backwards leaving enough time for the feeder to displace the raw material forward in the amount of uniform cutting thickness.

The design of the slider-crank mechanism performing cutting process at an average constant slider speed between the identified cutting positions of the raw material has been realized in [2] as a kinematic synthesis problem, since acceleration-free slider motion is necessary for a smooth cutting operation. For the stated purpose, the recti-linear slider displacement in some part of the mechanism motion is required to be a linear function of the crank angular displacement in that study [2]. How a desirable constant pushing force can be generated at varying crank positions under static conditions at contact phase in a feeder slider-crank mechanism has been explained in another work, [3]. On the other hand, in order to properly realize the required slider speeds and displacements during no-contact phase in such feeder mechanisms, recognizing their multi-body, time-dependent and non-linear characteristics of their motion, there is a need first to develop their dynamic model, and then to optimize their output. In this way, the problem can be viewed essentially as a control problem by which the feeder motion is regulated in the time-domain in accordance with the requirements of the process explained above. Within such a context, here in this work optimum conditions are explored for a cost-effective realization.

Although the slider position and speed control is involved in the design of the feeder slider-crank mechanism of the problem described above, in view of the fact that accuracy provided by an inexpensive open control would be sufficient here to satisfy the requirements of obtaining uniform ice particles, closed speed and position control solutions of the slider-crank mechanisms, abundant in literature [4, 5], are ruled out. Thus, in accordance with the principle of efficient use of resources in this control problem, after fulfilling the dynamic requirements of the process, the problem is reduced to finding the optimum values of the operating parameters of the feeder system. This, in turn, makes it necessary to formulate the dynamic equation of motion in its specific arrangement of the feeder slider-crank mechanism, which contains operating parameters to be subjected to an optimization process.

There are works in the literature which kinematically aim at finding the optimum values of the parameters pertaining to their specific systems. For instance, by neglecting gravitational and inertial effects in [6] the best transmission angle, maximum mechanical advantage and minimum error of input/output linearity have been shown in an inverted slider-crank (RPRR) mechanism, where slider is used as oscillating-slide actuator. In [7], Hooke-Jeeves optimization method has been applied to realize the synthesis of a four-bar mechanism in which the coupler point follows a rectilinear trajectory with controlled deviations.

There are also works in the literature which aim at improving the dynamic performance of the conventional slider-crank mechanisms. For example, dynamic model of slider-crank mechanism in two-cylinder compressor is utilized in topology optimization of crankshaft weight reduction [8]. In another example, dynamic model of a slider-crank mechanism with a linear spring and damper on the piston is used for observing the response of the system when an intermittent linear actuating force is applied on the piston [9].

It is obvious that optimization methods play significant roles in the cost-effective realization of the feeder problem described above. From among the available optimization methods in the literature, Hooke-Jeeves direct search method [10], consistent with the dominantly numerical character of this research, has been selected as the most suitable one for the non-linear optimization to be implemented in this study. Thus, a review of basic literature on Hooke-Jeeves direct search method appears to be in order here. Within this context, Wu et al. [11] applied Hooke-Jeeves optimization method to the calibration of seven soot model parameters used in the model of soot formation and oxidation in diesel engines. Mazouz et al. [12] showed application of Hooke-Jeeves method for the optimization of PI regulator gains in offshore wind energy production with permanent magnet synchronous generator. Benasla et al. [13] presented the application of Hooke-Jeeves method for the fuel cost minimization in power generation (i.e., economic dispatch problem).

In addition to application of original Hooke-Jeeves optimization method, various modified Hooke-Jeeves methods as well as hybrid application of this method involving other optimization methods have been presented. For instance, Li and Rahman [14] suggested a modification to Hooke-Jeeves optimization method by applying pattern move immediately after a successful pattern move instead of an exploratory move first to maintain the movement in the optimum direction. Litvinas [15] utilized a hybrid optimization of Bayesian-based global search supported with Hooke-Jeeves local search for multi-objective optimization. In that study, the multi-objective problem was reduced to a single objective problem during the application of Hooke-Jeeves method for local refinement process. Alkhamis et al. [16] used modified Hooke-Jeeves method to stochastic simulation results such that the confidence intervals associated with point estimate of the objective function are optimized. Tabassum et al. [17] presented hybrid application of genetic algorithm and Hooke-Jeeves method to the optimization of economic load dispatch problems with equality constraints.

In all these studies on Hooke-Jeeves optimization method [11–17], it is commonly shared that (i) an increment amount is randomly defined for exploratory search by the user; (ii) a multiplier of one is taken for the pattern move from the base point; (iii) the process is stopped as soon as no move is established by repeatedly dividing the increment amount, which may not make sure that optimization objective is mathematically achieved. However, all these quantities mentioned above are numerically determined here in this work on a mathematical basis such that finally the difference between the actual and desired objects, referred to as the objective function, is practically zero, implying to the achievement of optimum.

To the best of authors' knowledge, there is no other work in the literature that addresses itself essentially as an economic and simple solution to the problem of obtaining required uniform slider motion over a time domain or required speeds and displacements in desired time intervals in feeder slider-crank mechanisms. The main contribution of this work is an integrated process by which selected parameters of a given feeder slider-crank mechanism are optimized to satisfy the desired objectives. In the first stage of this process presented in Sections 2 and 8, the dynamic model of the slider-crank mechanism operating under special circumstances has had to be developed and the resulting non-linear differential equation has had to be solved by numerical methods. Based on the output of this dynamic model, the optimization of the selected parameters has been realized by a modified Hooke-Jeeves Method through a particular procedure developed, as described in Section 3. The basic novelty involved in the modified Hooke-Jeeves method is the procedure by which a cost-effective advancement towards a target optimum point is accomplished in a very short time. A user-friendly interface has been set up to support the optimization procedure, in Section 4. A numerical example is presented to illustrate the procedure, in Section 5. Validation of the results thus obtained has been demonstrated, in Section 6 together with conclusions in Section 7.

2. Theory

The slider-crank mechanism used as a feeder, shown with all of its parameters in Fig. 2, is the subject of this study. In this design, forward translational motion of the slider (C) is secured by a constant force (F_B) parallel to the gravitational acceleration (g) and a lumped mass (m_B) applied at the crank-connecting rod joint centre (B). The rotational spring attached to the crank at its center (O) is assumed to have a suitable spring constant (k) evaluated according to a required output/input force ratio [3]. When the mechanism is set to motion at a particular position for feeding raw material, the slider will develop, in general, a non-linear motion involving positions and speeds varying with time. Hence, the problem is how to optimize selected operating parameters so that a desired uniform slider speed within a desired displacement can be obtained such that feed rate can practically be kept at a constant level under a predetermined error value.

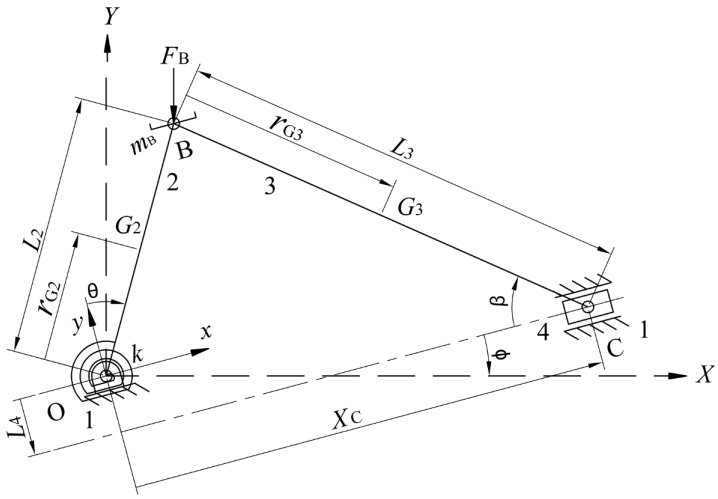

Fig. 2. Slider-crank mechanism parameters

In Fig. 2, the physical dimensions of the mechanism characterizing the lengths and the centers of gravity of moving arms, crank (2), connecting rod (3) are L_2, L_3 and r_{G2}, r_{G3}, respectively while the eccentricity between the slider (4) line of motion and the crank center (O) is designated by L_4. Crank, connecting rod, slider masses are symbolized by m_2, m_3 and m_4, respectively while the mass-moment-of-inertias for crank and connecting rod are represented by I_{G2} and I_{G3}, respectively. The symbols θ and β designate independent crank angle and dependent connecting rod angle, respectively, with corresponding sign conventions (both measured positive clockwise). F_B represents the constant basic external load applied to secure motion while m_B stands for externally added mass at point B having both static (i.e., gravitational) and dynamic (i.e., inertial) effects. Sliding friction between the ground and slider is taken into account by the coefficient of friction μ. The parameter ϕ defined as the angle between the horizontal and the sliding axes is introduced to enhance the scope of applications. In Fig. 2, "X–Y" coordinate system located at the crank center (point O) represents the horizontal and vertical reference axes, while "x–y" coordinate system located also at the crank center is defined by "x-axis" parallel to the slider sliding direction and "y-axis" perpendicular to it. Hence, the raw material being loaded in front of slider, crank being positioned at an initial angle θ_0 and the spring suitably acting on the crank, the system is driven by the application of a suitable external force F_B coupled with the suitable mass m_B effect for feeding the raw material in the direction of "x-axis".

Dynamic model of the feeder system described above is derived in the appendix and is given in the form of a second order non-linear differential equation as shown below:

$$A_2(\theta)\ddot{\theta} + A_1(\theta)\dot{\theta}^2 + A_0(\theta) = 0, \tag{1}$$

where A_2, A_1, A_0 are variable coefficients defined in the Appendix.

From among the possible direct numerical methods, the so-called 4-th order Runge-Kutta Method [18] has appeared to be well-suited to the solution of Eq. (1) with assigned conditions of initial crank angle (θ_0) and initial crank angular speed (ω_0). It should be added that this method yields low truncation error, in the order of $O(h^5)$ where h is the step size, and better accuracy when compared with other alternatives.

It is neccesary to underline tacit assumptions made in this section, as crank need to start motion at most from a vertical position and end its motion when the slider speed approaches zero and that the slider has only, whenever required, a unidirectional forward displacement. Furthermore, initial crank position (θ_0) should at least be equal to or larger than spring neutral position (θ_0^*).

3. Optimization of operation parameters

3.1. Preliminaries

A readily available slider-crank mechanism has the design parameters such as L_2, L_3, L_4, r_{G2}, r_{G3}, m_2, m_3, m_4, I_{G2} and I_{G3}, which are all fixed. The angle ϕ between the horizontal and the sliding axes as well as the coefficient of friction μ between the slider and ground have not been regarded as practically controllable parameters; they have been considered as application-dependent parameters and thus they have been kept fixed for the application at hand. Hence, five operating parameters (F_B, m_B, k, θ_0^* and θ_0) which can easily be implemented during the operation of the system have been selected as parameters to be optimized to yield the desired average slider speed over a predetermined displacement.

Recalling that the required energy to actuate the slider-crank mechanism is provided by the vertical force and lumped mass applied at point B, a forward feeding is to be satisfied under the following geometric constraints (Fig. 2):

$$\phi < \theta < \phi + 90, \tag{2}$$

$$\sin^{-1}\left(\frac{L_4}{L_2+L_3}\right) < \beta < \sin^{-1}\left(\frac{L_2\cos\phi + L_4}{L_3}\right), \tag{3}$$

$$\theta_{\max} = 90 + \sin^{-1}\left(\frac{L_4}{L_2+L_3}\right), \tag{4}$$

$$\theta_0 > \phi, \tag{5}$$

$$\theta_0 \geq \theta_0^*, \tag{6}$$

$$L_2\sin\phi + \left[L_3^2 - (L_2\cos\theta_0 + L_4)^2\right]^{1/2} < X_C < \left[(L_2+L_3)^2 - L_4^2\right]^{1/2}. \tag{7}$$

The slider velocity against its position, from the start to the end of its motion, in the mechanism of Fig. 2, can graphically be represented as depicted in Fig. 3.

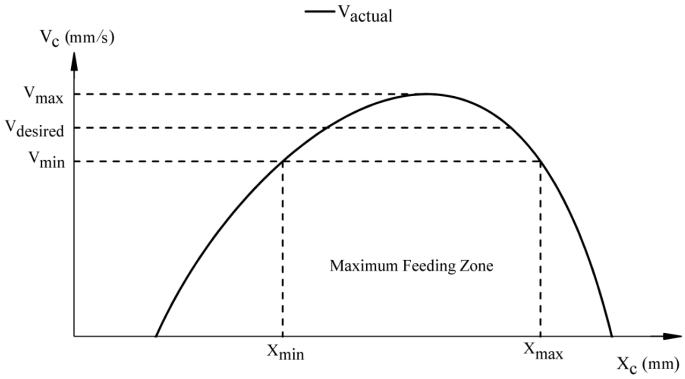

Fig. 3. Graphical representation of slider speed vs. slider position

Since the feeding has to be performed at a particular uniform speed, a theoretical error (e_{theo}) relationship can be defined between the minimum ($V_{\min}$), maximum ($V_{\max}$) feeding slider speeds and a desired feeding speed ($V_{\text{desired ave}}$) as:

$$e_{\text{theo}} = \frac{V_{\max} - V_{\min}}{V_{\text{desired ave}}} . \tag{8}$$

In this way, the variable error can be confined to a desirable value set at (e_{theo}). For an estimation purpose, it is suitable to rewrite Eq. (8) in the form of theoretical maximum ($(V_{\max})_{\text{theo}}$) and theoretical minimum ($(V_{\min})_{\text{theo}}$) speeds as follows:

$$(V_{\max})_{\text{theo}} = (2 + e_{\text{theo}}) \frac{V_{\text{desired ave}}}{2} , \tag{9}$$

$$(V_{\min})_{\text{theo}} = (2 - e_{\text{theo}}) \frac{V_{\text{desired ave}}}{2} . \tag{10}$$

Since an optimization process to be selected in conformity with the numerical nature of the problem will require a series of iterations, the maximum actual speed, on the other hand, has to be obtained from the solution of the governing differential equation of Eq. (1) with the corresponding design and operating parameters for each iteration. By representing the operating parameters of F_B, m_B, k, θ_0^*, θ_0 with $\boldsymbol{Y}^i = \left[y_1^i, y_2^i, y_3^i, y_4^i, y_5^i\right]$, respectively, actual maximum speed, $V_{\text{act}}^i\{\boldsymbol{Y}^i\}$, evaluated with y_j^i ($j = 1{-}5$) parameter value at i-th iteration step is defined as follows:

$$V_{\text{act}}^i \left\{\boldsymbol{Y}^i\right\} = \max \left\{\dot{X}_C^i(t_0),\ \dot{X}_C^i(t_1),\ \ldots,\ \dot{X}_C^i(t_n)\right\} , \tag{11}$$

where slider speeds $\dot{X}_C^i(t_k)$ are evaluated at time (t_k), k varying from 0 to n, at i-th iteration step.

For optimization purposes, an actual error e_{act}^i is defined as follows:

$$e_{\text{act}}^i = \frac{V_{\text{act}}^i \left\{\boldsymbol{Y}^i\right\} - (V_{\max})_{\text{theo}}}{(V_{\max})_{\text{theo}}} . \tag{12}$$

Once the operating parameters are optimized to yield the *unique* theoretical maximum slider speed, it will be possible to directly determine the two slider positions (i.e., $X_{\min}$ and $X_{\max}$ in Fig. 3) and hence the theoretical slider displacement (i.e., $\Delta X_C = X_{\max} - X_{\min}$, the maximum feeding zone) corresponding to the *theoretical minimum speed*, calculated by Eq. (10), as is evident from the curve of Fig. 3. However, this *theoretical minimum speed* may not match the desired slider displacement. In that case, in order to find out the *actual minimum speed* corresponding to the desired slider displacement (feeding span), a quadratic curve is fitted, through regression, with the available actual data resulting from the solution of the nonlinear equation in the *maximum feeding zone*. Using the equation of fitted quadratic curve, the minimum slider position (X_{min}) and the actual minimum speed value will be determined such that the quadratic curve gives the same minimum speed value at $X_{\max}$ and at $X_{\min}$, where the difference ($X_{\max} - X_{\min}$) is set equal to the desired slider displacement.

In order to assess the optimum result, definition of error (e_V) at the slider speed given below will be used to see deviation of the *actual* slider speed ($\dot{X}_C(t_k)$)) from the *specified* average speed ($V_{\text{desired ave}}$) at each slider position inside the given displacement domain.

$$e_V = \frac{\dot{X}_C(t) - V_{\text{desired ave}}}{V_{\text{desired ave}}} \,. \tag{13}$$

3.2. Modified Hooke-Jeeves optimization method

It is observed that Hooke-Jeeves method is essentially a direct numerical optimization method, which has been reliably and extensively implemented in many industrial problems such as these [11–17, 19]. Due to the fact that numerical data are available from the numerical solutions of a highly non-linear differential equation, minimization of the errors defined previously requires the use of a commensurate method. In this regard, Hooke-Jeeves method has appeared to be very well-suited to the problem in question. It is necessary to note that unlike the semi-analytical methods such as Taylor's series expansion [10, 20], whereby the higher order derivatives of the objective function, which significantly increase the volume of computations, are not analytically needed here. Moreover, the unique way by which the objective function is defined (i.e., Eqs. (11), (12)) does not provide any convenient basis for such approaches.

Hooke-Jeeves method has basically two steps for the error minimization process: one being a search for a suitable set of increment values for the parameters subject to change to indicate a unit step size in the desired direction and the other being to move by multiples of the unit step size to affect a considerable reduction in error. A suitable set of increment values is found by incrementing/decrementing each parameter by an amount (Δy_j) until a decrease in actual error value is satisfied

as follows:

$$y_j^{i+1} = \begin{cases} y_j^i + \Delta y_j\,, & \text{if } e_{\text{act}}^{i+1} < e_{\text{act}}^i\,, \\ y_j^i - \Delta y_j\,, & \text{if } e_{\text{act}}^{i+1} < e_{\text{act}}^i\,, \\ y_j^i\,, & \text{if } e_{\text{act}}^{i+1} \geqslant e_{\text{act}}^i \end{cases} \qquad j = 1, \ldots, 5, \tag{14}$$

$$\Delta y_j = y_j^{i+1} - y_j^i, \quad j = 1, \ldots, 5. \tag{15}$$

These increments (Δy_j) are user defined in the regular method and the amount of reduction in error for each increment depends on the value of the increment. Also, if an error reduction is achieved in the first iteration of increasing an operating parameter by an increment amount (Δy_j) in Eq. (14), then the second iteration of decreasing the same operating parameter by an increment amount (Δy_j) is not tried. If neither increasing nor decreasing an operating parameter reduces the error then the corresponding operating parameter (Δy_j) is kept at the same level. In this way, the increment vector is formed as such:

$$\boldsymbol{\Delta Y} = [\Delta y_1,\ \Delta y_2,\ \Delta y_3,\ \Delta y_4,\ \Delta y_5]\,. \tag{16}$$

The user defined increments (Δy_j) directly affect the state whether or not optimized operating parameter values are eventually to be secured, or how many or more iterations will be run to that end. This means that differently selected user defined increment (Δy_j) amounts, for the same initial operating parameters, can yield completely different results. Thus, this selection has to be standardized by finding the amount of increments that will cause unit change at maximum speed.

One of the novelties contributed to the Hooke-Jeeves pattern search is the selection of the values of the parameters involved in the increment vector $\Delta \boldsymbol{Y}$. Within this context, finite difference between the actual maximum speed values corresponding to a change of (Δy_j) in one parameter y_j is considered to numerically calculate the partial derivative of actual maximum speed with respect to each individual operating parameter ($\partial V_{\text{act}}^{i+j} / \partial y_j$) by the following formula:

$$\frac{\partial V_{\text{act}}^{i+j}}{\partial y_j} = \frac{V_{\text{act}}^i \left\{ y_j^i + \Delta y_j \right\} - V_{\text{act}}^i \left\{ y_j^i \right\}}{\Delta y_j}\,, \qquad j = 1, \ldots, 5. \tag{17}$$

Using this value, the increment (Δy_j), by which each parameter is changed, corresponding to a unitary change in the actual error value is determined according to following relation:

$$\Delta y_j = \frac{1}{\left(\partial V_{\text{act}}^{i+j} / \partial y_j \right)}\,. \tag{18}$$

Since the sets of values in Eq. (16) are determined on a magnitude basis to reduce error defined by Eq. (12) in the absolute sense, the direction to move closer to the target point should take into account where the value of $V_{\text{act}}^i\{\boldsymbol{Y}^i\}$ stands with

respect to the value of $(V_{\max})_{\text{theo}}$ at any iteration step. Thus, instead of iterating Eqs. (14)–(15) for increment vector given by Eq. (16), it will be directly determined by Eq. (19), whereby Δy_j values are calculated by Eq. (18):

$$\Delta \boldsymbol{Y} = -\text{sign}\left(e^i_{\text{act}}\right)\left[\Delta y_1,\ \Delta y_2,\ \Delta y_3,\ \Delta y_4,\ \Delta y_5\right], \tag{19}$$

where

$$\text{sign}\left(e^i_{\text{act}}\right) = \begin{cases} +1, & \text{if } V^i_{\text{act}} > (V_{\max})_{\text{theo}}\ , \\ -1, & \text{if } V^i_{\text{act}} < (V_{\max})_{\text{theo}}\ . \end{cases} \tag{20}$$

Once the correct direction is determined on a unitary basis, the next step is to estimate a positive multiplier λ^i by which a point potentially closer to the target point is reached as follows:

$$\boldsymbol{Y}^{k+1} = \boldsymbol{Y}^{i-5} + \lambda^k \Delta \boldsymbol{Y}, \quad k = i,\ i{+}1,\ i{+}2,\ i{+}3, \ldots,\ \ i \geqslant 5. \tag{21}$$

$\boldsymbol{Y}^{i-5}$ in Eq. (21) represents the point of operating parameters for which the increment vector $(\Delta \boldsymbol{Y})$ is calculated based on Eqs. (15) and (19).

Another novelty contributed to the Hooke-Jeeves pattern search is to be found in the estimation of multiplier λ^i. The idea by which a suitable multiplier is determined for cost effective optimization is based on forcing the error defined in Eq. (12) to zero in two consecutive steps. In the first step, multiplier λ^k values are set to $(\lambda^i = 1)$ and $(\lambda^{i+1} = 1.5)$ in Eq. (21) to find $\boldsymbol{Y}^{i+1}$ and $\boldsymbol{Y}^{i+2}$. Errors e^{i+1}_{act} and e^{i+2}_{act} corresponding to $\boldsymbol{Y}^{i+1}$ and $\boldsymbol{Y}^{i+2}$, respectively are found by reference to Eq. (12). By extrapolation using pairs of points $(\lambda^i, e^{i+1}_{\text{act}})$ and $(\lambda^{i+1}, e^{i+2}_{\text{act}})$, the suitable λ^{i+2} value is calculated for $e^{i+3}_{\text{act}} = 0$ as follows:

$$\lambda^{i+2} = \lambda^i + \left(-e^{i+1}_{\text{act}}\right) \frac{\lambda^{i+1} - \lambda^i}{e^{i+2}_{\text{act}} - e^{i+1}_{\text{act}}}\ . \tag{22}$$

Then, operating parameters $\boldsymbol{Y}^{i+3}$ are found by substituting λ^{i+2} in Eq. (21), followed by calculation of the actual error e^{i+3}_{act} by means of Eq. (12). In case any negative operating parameters are encountered in $\boldsymbol{Y}^{i+3}$, the latest multiplier λ^{i+2} value is taken half of itself and the new operating parameter set $(\boldsymbol{Y}^{i+3})$ is determined by means of Eq. (21) assuring all non-negative operating parameter set. Although the aim of the first step is making the error e^{i+3}_{act} zero, it does not factually make the error zero. Thus, the idea of forcing the error e^{i+4}_{act} to zero will be continued in the second step. Although in the second step the error may not end in zero value, it will certainly provide the new multiplier that will cause a reduction in the error. It should be noted that interpolation implies a sign change in error while extrapolation indicates to the same sign in error. To that end, an interpolation or extrapolation is carried out between the pairs of $(\lambda^{i+1}, e^{i+2}_{\text{act}})$ and $(\lambda^{i+2}, e^{i+3}_{\text{act}})$ to find the pair $(\lambda^{i+3}, e^{i+4}_{\text{act}})$ such that e^{i+4}_{act} will be zero:

$$\lambda^{i+3} = \lambda^{i+2} + \left(-e^{i+3}_{\text{act}}\right) \frac{\lambda^{i+2} - \lambda^{i+1}}{e^{i+3}_{\text{act}} - e^{i+2}_{\text{act}}}\ . \tag{23}$$

Final novel contribution to the Hooke-Jeeves pattern search can be mentioned in improving the efficiency of calculations i.e., forcing zero error on finite difference of the maximum speed with respect to the change *only* in force F_b (i.e., y_1) value when the actual error (e^i_{act}) gets values less than 0.01. It is observed that when navigating around small error levels (i.e., when $e^i_{\text{act}} < 0.01$ the process generally wastes too many iterations before reaching optimum results. Therefore, the necessary value of force F_b (y_1^{i+1}) corresponding to error level (e^{i+1}_{act}) value of zero is then calculated, by keeping the rest four operating parameters fixed, as follows:

$$y_1^{i+1} = y_1^i + e^i_{\text{act}} \Delta y_1 \,. \tag{24}$$

3.3. Optimization procedure

The following series of steps have come out as an appropriate procedure by which optimum values of the operating parameters in question are determined:

1. Enter the parameters L_2, L_3, L_4, r_{G2}, r_{G3}, m_2, m_3, m_4, I_{G2}, I_{G3}, ϕ and μ.
2. Enter the desired feeding speed ($V_{\text{desired ave}}$) as well as the allowable speed error e_{theo}.
3. Calculate $(V_{\max})_{\text{theo}}$ and $(V_{\min})_{\text{theo}}$ from Eqs. (9) and (10).
4. For $i = 0$, define $k = i$ and choose an initial point for operating parameters $\boldsymbol{Y}^0 = \left[y_1^0, y_2^0, y_3^0, y_4^0, y_5^0\right]$ that satisfies the constraints of Eqs. (2)–(7).
5. Solve the governing differential equation Eq. (1).
6. Find the maximum speed $V^i_{\text{act}}\{\boldsymbol{Y}^i\}$ and the actual error e^i_{act} by Eqs. (11) and (12).
7. **If** $\left\{\left|e^i_{\text{act}}\right| < 0.00001\right\}$ then $\boldsymbol{Y}_{\text{optimized}} = \boldsymbol{Y}^i$ and go to Step 22.
8. **If** $\left\{\left|e^i_{\text{act}}\right| \geq 0.01\right\}$ then **If** $\{k = i$ then go to Step 9$\}$ or $\{k = i + 1$ then go to Step 13$\}$ or $\{k = i + 2$ then go to Step 16$\}$ or $\{k = i + 3$ then go to Step 20$\}$.
   a. Calculate the necessary increment amount (Δy_1) and the new force (y_1^{i+1}) by Eq. (24).
   b. With the new $\boldsymbol{Y}^{i+1}$, calculate the actual error e^{i+1}_{act}.
   c. **If** $\{\left|e^i_{\text{act}}\right| < 0.00001\}$ then $\boldsymbol{Y}_{\text{optimized}} = \boldsymbol{Y}^{i+1}$ and go to Step 22.
9. For $i = i + j$, $j = 1, 2, \ldots, 5$ find increment amount (Δy_j) corresponding to a unitary change in the actual error value by Eqs. (17) and (18).
10. Find increment vector $\Delta \boldsymbol{Y}$ of the modified Hooke-Jeeves method by Eq. (19).
11. For $\lambda^i = 1$ define $k = i + 1$ and calculate $\boldsymbol{Y}^{i+1}$ by Eq. (21).
12. Go to Step 5 with $\boldsymbol{Y}^{i+1}$ values.
13. For $\lambda^{i+1} = 1.5$, define $k = i + 2$.
14. Calculate $\boldsymbol{Y}^{i+2}$ for λ^{i+1} by Eq. (21).
15. Go to Step 5 with $\boldsymbol{Y}^{i+2}$ values.
16. If $\left\{\text{sign}\left(e^{i+1}_{\text{act}}\right) \neq \text{sign}\left(e^{i+2}_{\text{act}}\right)\right\}$
    calculate a new λ^{i+3} for $e^{i+4}_{\text{act}} = 0$ by interpolating or extrapolating.
    Else calculate λ^{i+2} value by Eq. (22).

17. Define $k = i + 3$ and calculate $\boldsymbol{Y}^{i+3}$ for λ^{i+2} by Eq. (22).
18. **If** {any value of $\boldsymbol{Y}^{i+3}$ is less than zero} then
choose a new $\lambda^{i+3} = \lambda^{i+2}/2$ such that $\{\boldsymbol{Y}^{i+4}\}$ have non-negative values for each operating parameter.
19. Go to Step 5 with $\boldsymbol{Y}^{i+4}$ values.
20. **If** $\{i \geqslant 100000\}$ then go to step 4 (i.e., choose a new initial point for operating parameters $\boldsymbol{Y}^{i}$).
21. Define $k = i$ and go to Step 9 with the latest $\boldsymbol{Y}^{i}$ operating parameters.
22. End

4. Development of user interface

In order to free the user's mind off the background details and to direct his or her attention more onto the input-output relationships for a conveniently implementable result, an interface is developed written in Visual Basic language, and shown in Fig. 4.

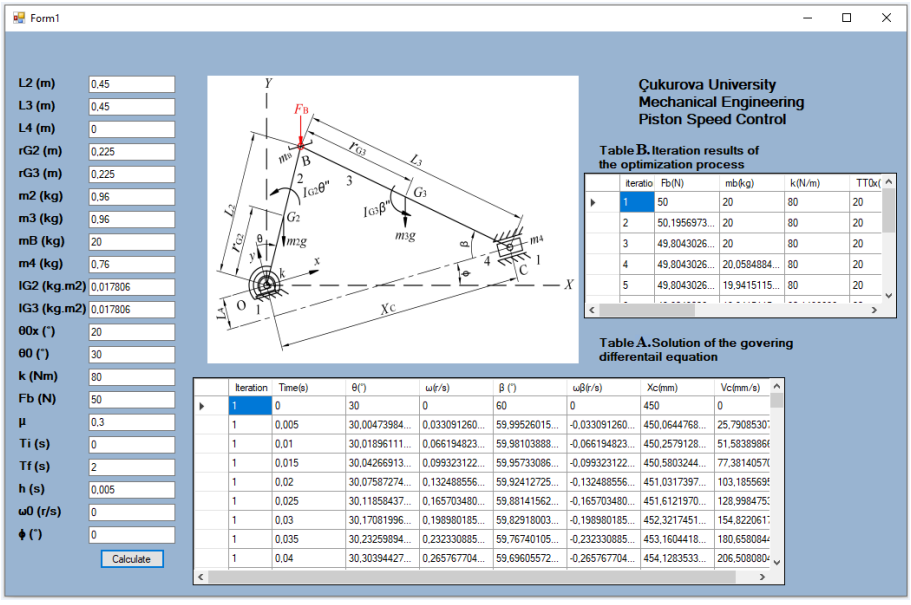

Fig. 4. The user interface of position-speed calculations in slider-crank feeder mechanism

Input (a total of 18 parameters that appear in the mathematical model) as well as numerical solution parameters of initial time (T_i), final time (T_f) and discrete time interval (h) are entered to the user interface in Fig. 4 through the boxes on its left-hand side. Following the entry of all the parameters, outputs from the user interface are obtained as the numerical values of crank position, crank angular speed, connecting link position, connecting link angular speed, slider position and

slider speed in terms of time increments, which result from the solution of the differential equation as well as from the associated equations for each individual iteration, in a table at the bottom (Table A – Fig. 4) simultaneously transferring them to an Excel worksheet. Also, the operation parameters (F_B, m_B, k, θ_0^*, θ_0) together with the resulting actual maximum slider position and speed as well as the actual error for each individual iteration are collected in a second table (Table B – Fig. 4) simultaneously transferring them to an Excel worksheet, too. Hence, the optimized operating parameters can be read directly from Table B of the user interface whereas individual solutions of each iteration can be found in Table A of the user interface with respect to the corresponding iteration number.

5. Numerical example

The optimization procedure integrating all the elements mentioned so far, i.e., the mathematical model of the mechanism, its numerical solution, constraints and modified form of Hooke-Jeeves pattern search is applied on a slider-crank mechanism which is described by the data given in Table 1. The slider is desired to move with a uniform speed of 0.9 m/s over a 0.09 m displacement with a maximum allowable error of 5%. Therefore, the maximum and minimum theoretical speeds which are required to be attained in the optimization process are 0.9225 m/s and 0.8775 m/s, respectively.

Table 1. Design parameters for example slider-crank mechanism

L_2 (m)	0.4500	m_2 (kg)	0.9600
L_3 (m)	0.4500	m_3 (kg)	0.9600
L_4 (m)	0.0000	m_4 (kg)	0.7600
r_{G2} (m)	0.2250	I_{G2} (kg m^2)	0.0178
r_{G3} (m)	0.2250	I_{G3} (kg m^2)	0.0178
ϕ (°)	0.0000	μ	0.3000

Against an initial solution satisfying the geometric constraints of Eqs. (2)–(7), the results of modified Hooke-Jeeves method optimization process have been collected in Table 2. Totally 19 iterations have been sufficient to optimize the operating parameters.

In Table 2, the extrapolated multiplier value (λ^7) for the 8$^{\text{th}}$ iteration results in a change of sign in error. Hence, a new multiplier value (λ^8) has been interpolated. The iteration yields a reduction in error with the same sign. The procedure is continued. At the 18$^{\text{th}}$ iteration, the operating parameters yield an error of 0.033%, which is less than 1%, as the limit determined in the procedures for fine-tuning force F_B. Hence, the necessary change in the force to make the actual error zero is calculated as $\Delta F_B = -0.036$ N. This change reduces the actual error to a value of 3.1E-05% which is less than 0.001% that is the limit to stop iteration.

Table 2. Optimized operating parameters for example slider-crank mechanism

	F_B (N)	m_B (kg)	k (Nm)	θ_0^* (°)	θ_0 (°)	$\boldsymbol{V}^i_{\text{act}}\{\boldsymbol{Y}^i\}$ (m/s)	e^i_{act} (%)
$\boldsymbol{Y}^0$	50.000	20.000	80.000	20.000	30.000	1.4410	56.204
$\Delta\boldsymbol{Y}$ (Inc. Vector)	–0.196	–0.058	0.149	–0.042	0.038		
For $\lambda^5 = 1$; $\boldsymbol{Y}^6$	49.804	19.942	80.149	19.958	30.038	1.4358	55.641
For $\lambda^6 = 1.5$; $\boldsymbol{Y}^7$	49.706	19.912	80.223	19.937	30.057	1.4332	55.358
For $\lambda^7 = 99.410$; $\boldsymbol{Y}^8$	30.546	14.186	94.779	15.802	33.745	0.5957	-35.427
For $\lambda^8 = 61.203$; $\boldsymbol{Y}^9$	38.023	16.420	89.099	17.415	32.306	1.0354	12.236
$\Delta\boldsymbol{Y}$ (Inc. Vector)	–0.129	–0.020	0.088	–0.025	0.039		
For $\lambda^{14} = 1$; $\boldsymbol{Y}^{15}$	37.894	16.400	89.187	17.390	32.345	1.0304	11.692
For $\lambda^{15} = 1.5$; $\boldsymbol{Y}^{16}$	37.829	16.390	89.231	17.377	32.365	1.0278	11.418
For $\lambda^{16} = 22.344$; $\boldsymbol{Y}^{17}$	35.141	15.971	91.067	16.850	33.184	0.9169	–0.608
For $\lambda^{17} = 21.289$; $\boldsymbol{Y}^{18}$	35.277	15.993	90.974	16.876	33.143	0.9228	0.033
$\Delta\boldsymbol{Y}$ (Inc. Vector)	–0.036	–	–	–	–		
$\boldsymbol{Y}^{19}$	35.241	15.993	90.974	16.876	33.143	0.9225	3.1E-05

As a final step, a graph of V_C vs. X_C is drawn from the solution of the last iteration listed in Table A for the optimized operating parameters listed in Table B of the user interface. In this way, a displacement value of 0.1174 m for the maximum feeding zone is found in between two slider positions corresponding to the theoretical minimum speed. For the required feeding displacement of 0.09 m, a quadratic curve is fitted with the actual data of the maximum feeding zone as follows:

$$V_C = -0.013X_C^2 + 18.598X_C - 5725.4 \quad \text{where} \quad R^2 = 0.9986. \tag{25}$$

From the equation of the curve (Eq. (25)), the minimum slider position and minimum slider speed value are calculated as 0.6703 m and 0.8959 m/s, respectively, for an exact feeding displacement of 0.09 m. Actual error (e_V) in slider speed ($\dot{X}_C$) with respect to the desired average speed of 0.9 m/s is drawn with respect to slider position in Fig. 5. In this figure, the maximum, minimum and corresponding average speed values of 0.9225 m/s, 0.8959 m/s and 0.9092 m/s as well as their corresponding actual error values of 2.5%, 1.024% and –0.452% are presented for the feeding zone in question, respectively.

From the example presented above, it can clearly be observed that the procedure yields the optimum result in a notably small number of iterations, which is an indication of effectiveness and efficiency of the proposed procedure. This observation can be explained by contributions made in different phases of the Hooke-Jeeves pattern search, namely how the increments are decided in the first step and how these increments are magnified by a suitable step size selection technique and how

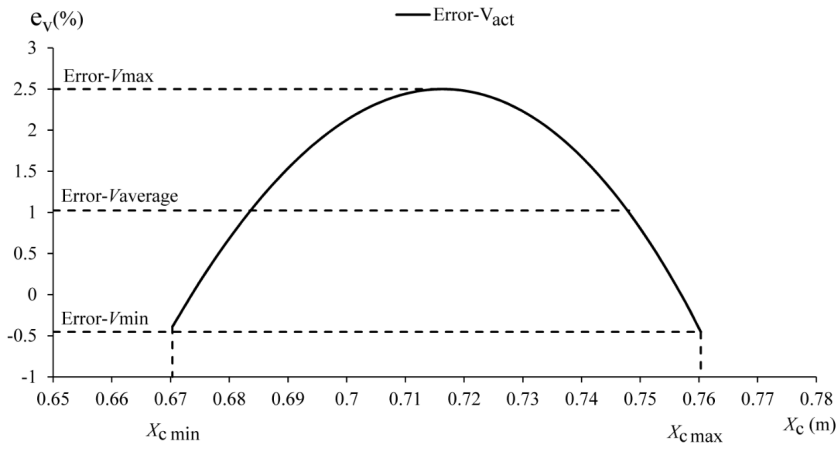

Fig. 5. Actual error in slider speed for the required feeding zone

in the final step the efficiency increase is ensured by reducing the number of variables of pattern search to a single one which has a physical meaning of being the major driving force of the dynamical system. From this observation, it is possible to characterize the solutions as energy-efficient due to the fact that smaller values of force (F_B) and added mass (m_B) are obtained by the procedure, as can clearly be seen from the results of example with respect to its initial values.

Curve fitting operation had to be applied following the optimization process, in order to adjust the optimization results to be consistent with the correct desirable feeding zone. However, this operation has modified the values of actual average and actual minimum slider speeds (Fig. 5). Nevertheless, these modifications, being limited in magnitude, do not cause the bounds to be exceeded and they never lead to higher values of error greater than the allowable error value.

6. Validation and simulation

The optimized dynamic model and the results therefrom are validated by the SolidWorks motion analysis tool. For comparison purposes, a solid model of a slider-crank mechanism is formed firstly based on the design parameters listed in Table 1 and the optimized operating parameters by the modified Hooke-Jeeves method listed in Table 2. The analysis is carried out and the result of slider speed vs. slider displacement is plotted. The depiction of the two results under the same parameter values, i.e., one from the SolidWorks designated by "SW-V_c" and the other from the developed user interface designated by "Int-V_c", is shown in Fig. 6, where the two resulting curves are observed to be in good agreement with each other.

At this point, it could be misleadingly thought that the optimized operating parameters would be simply obtained by several analyses in the SolidWorks motion

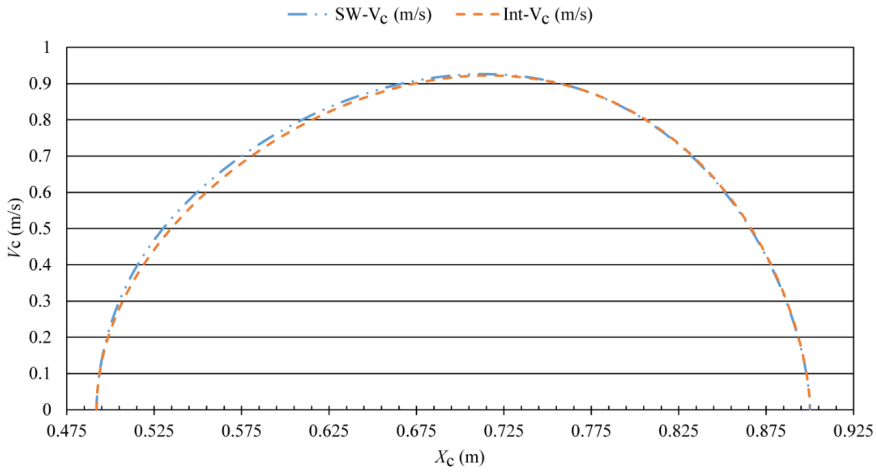

Fig. 6. Comparison of slider position vs. speed values

analysis tool. However, the optimization of the operating parameters cannot be guaranteed for controlling the motion under energy efficiency by using solid models and CAE software, since a trial-and-error method with CAE software will not provide any mathematical proof for optimum.

7. Conclusion

In this study, dynamic behavior of a slider-crank mechanism, which has a helical spring assembled on its crank and a constant force together with a lumped mass acting on its crank-connecting rod joint centre, has been modeled to realize the inexpensive open speed control of the slider over a predetermined slider displacement. A procedure for optimizing the proper values of operating parameters is devised. Then, the procedure has been illustrated on a particular example. Due to the repetitive character of calculations involved, a user interface has been instrumental in realizing the optimization objectives corresponding to a selected list of parameters. The results of the model developed in this work have also been proven to be in close agreement with a SolidWorks output.

Several contributions can be mentioned in obtaining energy-efficient operation of an available slider-crank mechanism supposed to act as a uniform-speed feeder providing controlled slider velocities over given domains. Primarily, the question as to how the optimum values of the driving forces, namely the magnitudes of the constant force and the inserted mass acting on the mechanism through the crank-coupler joint are to be attained finds its answers in this work. The results of this research also indicate how the optimum values of spring parameters, (i.e., spring constant, starting and neutral positions) associated with conceived feeder design of a slider-crank structure are to be determined to achieve the desired control objectives. The contributions cannot be fully explained without referring to the numerical

solution of the non-linear dynamic model of the conceived feeder mechanism, since the application of an effective optimization procedure is completely based on the numerical results of this dynamic model. Within this context, one of the novelties imbedded in the optimization process is the unique formation of an objective function formulated as a rational error function between the maximum of a numerical set and a single specified value, as displayed in Eqs. (11) and (12). Commensurate with the numerical nature of the optimization process here, the so-called Hooke-Jeeves method has been implemented to the problem in question in a modified form.

The basic novelty involved in the modified Hooke-Jeeves method is the procedure by which a cost-effective advancement towards a target optimum point is accomplished in a very short time. Instead of carrying out pattern search in arbitrary increments of parameters subject to change, the values of the increments are standardized in such a way that they are supposed to provide unit change in the desired direction of the unique maximum speed value. In this process, the increments have been calculated as the inverses of the partial derivatives of the optimization error function with respect to each parameter subject to change. Since abundant data are available from the solution of the differential equation of the dynamical system, these partial derivatives are approximated as the finite differences of the optimization error function with respect to each parameter subject to change. Another contribution is to be seen in determining the multiples of a suitable step size, which is obtained from the idea of forcing the error to zero. In view of the fact that advancement towards the optimum target point slows down as the process comes nearer to the target, computational burden is significantly reduced by basing the procedure on only the most effective single parameter, ending in the accelerated arrival at the optimum. Thus with all of these novel features, the overall efficiency of the classical Hooke-Jeeves optimization method, as implemented in this work, has been demonstrated to be improved.

Here in this work, the parameters subject to the optimization process have been limited only to those related with the direct operation of a feeder system assumed to be already available for direct implementation. However, it is worth noting that due to the abundance of parameters imbedded in the model it is possible to extend the optimization algorithm to other parameter sets as well, which may selectively include as many as 18 parameters.

8. Appendix A

From the free body diagrams of moving links, i.e., slider (4), connecting rod (3) and crank (2) in Fig. 2, D'Alembert equations are written, with reference to the x-y coordinate system attached to ground link (1), as follows:

$$F_{34x} - \mu F_{14} - m_4 \ddot{X}_C - m_4 g \sin\phi = 0, \tag{26}$$

$$F_{34y} + F_{14} - m_4 g \cos\phi = 0, \tag{27}$$

$$-F_{34x} + F_{23x} - m_3 a_{G3x} - m_3 g \sin\phi = 0, \tag{28}$$

$$-F_{34y} + F_{23y} - m_3 a_{G3y} - m_3 g \cos\phi = 0, \tag{29}$$

$$\begin{aligned} &-F_{34y} L_3 \cos\beta - F_{34x} L_3 \sin\beta - m_3 a_{G3y} r_{G3} \cos\beta - m_3 g \cos\phi r_{G3} \cos\beta \\ &\quad - m_3 g \sin\phi r_{G3} \sin\beta - m_3 a_{G3x} r_{G3} \sin\beta + I_{G3} \ddot{\beta} = 0, \end{aligned} \tag{30}$$

$$\begin{aligned} &-F_{23x} + F_{12x} - m_B L_2 \ddot{\theta} \cos\theta + m_B L_2 \dot{\theta}^2 \sin\theta - m_2 a_{G2x} \\ &\quad - F_B \sin\phi - m_B g \sin\phi - m_2 g \sin\phi = 0, \end{aligned} \tag{31}$$

$$\begin{aligned} &-F_{23y} + F_{12y} + m_B L_2 \ddot{\theta} \sin\theta + m_B L_2 \dot{\theta}^2 \cos\theta - F_B \cos\phi \\ &\quad - m_B g \cos\phi - m_2 a_{G2y} - m_2 g \cos\phi = 0, \end{aligned} \tag{32}$$

$$\begin{aligned} &T + m_B L_2^2 \ddot{\theta} + F_{23x} L_2 \cos\theta - F_{23y} L_2 \sin\theta - m_B g \cos\phi L_2 \sin\theta \\ &\quad + m_B g \sin\phi L_2 \cos\theta - F_B \cos\phi L_2 \sin\theta + F_B \sin\phi L_2 \cos\theta \\ &\quad - m_2 g \cos\phi r_{G2} \sin\theta + m_2 g \sin\phi r_{G2} \cos\theta + m_2 a_{G2x} r_{G2} \cos\theta \\ &\quad - m_2 a_{G2y} r_{G2} \sin\theta + I_{G2} \ddot{\theta} = 0. \end{aligned} \tag{33}$$

In equations (26) to (33), seven joint forces between the links of interest are represented by F_{12x}, F_{12y}, F_{23x}, F_{23y}, F_{34x}, F_{34y}, F_{14}; $\dot{\theta}$ and $\ddot{\theta}$ are crank angular speed and angular acceleration, respectively; $\ddot{\beta}$, g and $\ddot{X}_C$ are connecting rod angular, gravitational and slider linear accelerations, respectively; a_{G2x}, a_{G2y}, a_{G3x}, a_{G3y} are linear acceleration components along x, y axes associated with mass centers of crank (G_2) and connecting rod (G_3), respectively. Basic dependency relationships can typically be signified by equations (34) and (35) shown below:

$$\beta = \sin^{-1}\left[\frac{L_2 \cos\theta + L_4}{L_3}\right], \tag{34}$$

$$X_C = L_2 \sin\theta + L_3 \cos\beta. \tag{35}$$

It should be noted that the torque (T) induced on the crank by torsional spring in Eq. (33) is formulated in terms of the spring constant (k), crank angle (θ) and spring neutral angle for crank (θ_0^*) as such:

$$T = k\left(\theta - \theta_0^*\right) \quad \text{where} \quad \theta \geqslant \theta_0^*, \tag{36}$$

After eliminating all the joint forces and substituting the relevant joint force, torque, speed and acceleration quantities into equation (33) as well as collecting all the terms under common denominator $(L_3 \cos\beta - \mu L_3 \sin\beta)$, together with the condition that $(\mu \tan\beta)$ is different than 1, the following second order non-linear differential equation is obtained:

$$A_2(\theta)\ddot{\theta} + A_1(\theta)\dot{\theta}^2 + A_0(\theta) = 0, \tag{37}$$

where A_2, A_1, A_0 are variable coefficients defined below:

$$\begin{aligned}A_0(\theta) = {} & \left\{\left(L_3\cos\beta - \mu L_3\sin\beta\right)\left[k\left(\theta-\theta_0^*\right)\right]\right. \\ & + \cos\theta\cos\beta\left(m_B g\sin\phi L_2L_3 + F_B\sin\phi L_2L_3 + m_2 g\sin\phi r_{G2}L_3\right. \\ & \left. + \mu m_4 g\cos\phi L_2L_3 + \mu m_3 g\cos\phi r_{G3}L_2 + m_4 g\sin\phi L_2L_3 + m_3 g\sin\phi L_2L_3\right) \\ & + \sin\theta\cos\beta\left(-m_B g\cos\phi L_2L_3 - F_B\cos\phi L_2L_3 - m_2 g\cos\phi r_{G2}L_3\right. \\ & \left. + m_3 g\cos\phi r_{G3}L_2 - m_3 g\cos\phi L_2L_3\right) + \sin\theta\sin\beta\left(\mu m_B g\cos\phi L_2L_3\right. \\ & \left. + \mu F_B\cos\phi L_2L_3 + \mu m_2 g\cos\phi r_{G2}L_3 + \mu m_4 g\cos\phi L_2L_3 + m_4 g\sin\phi L_2L_3\right. \\ & \left. + m_3 g\sin\phi r_{G3}L_2 + \mu m_3 g\cos\phi L_2L_3\right) + \cos\theta\sin\beta\left(-\mu m_B g\sin\phi L_2L_3\right. \\ & \left. - \mu F_B\sin\phi L_2L_3 - \mu m_2 g\sin\phi r_{G2}L_3 + \mu m_4 g\sin\phi L_2L_3 + \mu m_3 g\sin\phi r_{G3}L_2\right. \\ & \left. - \mu m_4 g\sin\phi L_2L_3 - \mu m_3 g\sin\phi L_2L_3\right)\Big\}/\left(L_3\cos\beta - \mu L_3\sin\beta\right), \end{aligned} \tag{38}$$

$$\begin{aligned}A_1(\theta) = {} & \left\{\cos\theta\sin\theta\cos\beta\left(-m_4L_2^2L_3 - 2m_3r_{G3}L_2^2 + m_3r_{G3}^2\frac{L_2^2}{L_3}\right)\right. \\ & + \cos\theta\sin^2\theta\left(-m_4L_2^3 - m_3r_{G3}\frac{L_2^3}{L_3}\right) + \cos^2\theta\sin\beta\left(m_4L_2^2L_3\right. \\ & \left. + m_3r_{G3}L_2^2\right) + \cos\theta\sin^2\theta\sin^2\beta\sec^2\beta\left(-m_4L_2^3 - m_3r_{G3}\frac{L_2^3}{L_3}\right) \\ & + \cos\theta\sin^2\theta\sin\beta\sec\beta\left(-\mu m_3r_{G3}^2\frac{L_2^3}{L_3^2} + \mu m_3r_{G3}\frac{L_2^3}{L_3}\right) \\ & + \cos^2\theta\sin^2\beta\sec\beta\left(\mu m_3r_{G3}^2\frac{L_2^2}{L_3} - \mu m_3r_{G3}L_2^2\right) \\ & + \cos\theta\sin^2\theta\sin^3\beta\sec^3\beta\left(-\mu m_3r_{G3}^2\frac{L_2^3}{L_3^2} + \mu m_3r_{G3}\frac{L_2^3}{L_3}\right) \\ & + \cos^2\theta\cos\beta\left(-\mu m_3r_{G3}L_2^2 + \mu m_3r_{G3}^2\frac{L_2^2}{L_3}\right) \\ & + \mu I_{G3}\frac{L_2^2}{L_3}\cos^2\theta\sec\beta - \mu I_{G3}\frac{L_2^3}{L_3^2}\cos\theta\sin^2\theta\sin\beta\sec^3\beta \\ & + \sin^2\theta\sin\beta\left(-m_4L_2^2L_3 - m_3r_{G3}L_2^2\right) + \sin^3\theta\sin\beta\sec\beta\left(-m_4L_2^3\right. \\ & \left. - m_3r_{G3}^2\frac{L_2^3}{L_3^2}\right) + \cos\theta\sin\theta\sin^2\beta\sec\beta\left(m_4L_2^2L_3 + m_3r_{G3}^2\frac{L_2^2}{L_3}\right) \\ & + \sin^3\theta\sin^3\beta\sec^3\beta\left(-m_4L_2^3 - m_3r_{G3}^2\frac{L_2^3}{L_3^2}\right) + I_{G3}\frac{L_2^2}{L_3}\cos\theta\sin\theta\sec\beta \\ & \left. - I_{G3}\frac{L_2^3}{L_3^2}\sin^3\theta\sin\beta\sec^3\beta\right\}/\left(L_3\cos\beta - \mu L_3\sin\beta\right), \end{aligned} \tag{39}$$

$$
\begin{aligned}
A_2(\theta) = \Big\{ & \cos\beta \left(m_B L_2^2 L_3 + I_{G2} L_3 \right) + \sin\beta \left(-\mu m_B L_2^2 L_3 - \mu I_{G2} L_3 \right) \\
& + \cos^2\theta \cos\beta \left(m_4 L_2^2 L_3 + m_3 L_2^2 L_3 + m_2 r_{G2}^2 L_3 \right) \\
& + \cos^2\theta \sin\beta \left(\mu m_3 r_{G3} L_2^2 - \mu m_3 L_2^2 L_3 - \mu m_2 r_{G2}^2 L_3 \right) \\
& + \cos\theta \sin\theta \sin\beta \left(2 m_4 L_2^2 L_3 + 2 m_3 r_{G3} L_2^2 \right) \\
& + \cos\theta \sin\theta \sin^2\beta \sec\beta \left(\mu m_3 r_{G3}^2 \frac{L_2^2}{L_3} - \mu m_3 r_{G3} L_2^2 \right) \\
& + \cos\theta \sin\theta \cos\beta \left(-\mu m_3 r_{G3} L_2^2 + \mu m_3 r_{G3}^2 \frac{L_2^2}{L_3} \right) \\
& + \mu I_{G3} \frac{L_2^2}{L_3} \cos\theta \sin\theta \sec\beta + \sin^2\theta \cos\beta \Big(-2 m_3 r_{G3} L_2^2 \\
& + m_3 r_{G3}^2 \frac{L_2^2}{L_3} + m_3 L_2^2 L_3 + m_2 r_{G2}^2 L_3 \Big) + \sin^2\theta \sin\beta \big(- \mu m_3 L_2^2 L_3 \\
& + \mu m_3 r_{G3} L_2^2 - \mu m_2 r_{G2}^2 L_3 \big) + \sin^2\theta \sin^2\beta \sec\beta \left(m_4 L_2^2 L_3 + m_3 r_{G3}^2 \frac{L_2^2}{L_3} \right) \\
& + I_{G3} \frac{L_2^2}{L_3} \sin^2\theta \sec\beta \Big\} / \left(L_3 \cos\beta - \mu L_3 \sin\beta \right).
\end{aligned}
\tag{40}
$$

References

[1] M.I. Sarigecili and I.D. Akcali. Design of a uniform ice cutting device. In *Proceeding of the 2nd Cilicia International Symposium on Engineering and Technology (CISET 2019)*, pages 311–317, Mersin, Turkey, 10-12 October, 2019.

[2] İ.D. Akçalı and M.A. Arıoğlu. Geometric design of slider-crank mechanisms for desirable slider positions and velocities. *Forschung im Ingenieurwesen*, 75:61–71, 2011. doi: 10.1007/s10010-011-0134-7.

[3] M.I. Sarigecili and I.D. Akcali. Development of constant output-input force ratio in slider-crank mechanisms. *Inverse Problems in Science and Engineering*, 27(5):565–588, 2019. doi: 10.1080/17415977.2018.1470625.

[4] F. Ahmad, A.L. Hitam, K. Hudha, and H. Jamaluddin. Position tracking of slider crank mechanism using PID controller optimized by Ziegler Nichol's method. *Journal of Mechanical Engineering and Technology*, 3(2):27–41, 2011.

[5] C.D. Lee, C.W. Chuang, and C.C. Kao. Apply fuzzy PID rule to PDA based control of position control of slider crank mechanisms. In *Proceeding of the IEEE Conference on Cybernetics and Intelligent Systems*, pages 508–513, Singapore, 1-3 December, 2004. doi: 10.1109/ICCIS.2004.1460467.

[6] P.A. Simionescu. Optimum synthesis of oscillating slide actuators for mechatronic applications. *Journal of Computational Design and Engineering*, 5(2):215–231, 2018. doi: 10.1016/j.jcde.2017.09.002.

[7] R.R. Bulatović and S.R. Djordjević. Optimal synthesis of a four-bar linkage by method of controlled deviation. *Theoretical and Applied Mechanics*, 31(3-4):265–280, 2004. doi: 10.2298/TAM0404265B.

[8] A. Arshad, P. Cong, A.A.E. Elmenshawy, and I. Blumbergs. Design optimization for the weight reduction of 2-cylinder reciprocating compressor crankshaft. *Archive of Mechanical Engineering*, 68(4):449–471, 2021. doi: 10.24425/ame.2021.139311.

[9] J. Beckers, T. Verstraten, B. Verrelst, F. Contino, and J.V. Mierlo. Analysis of the dynamics of a slider-crank mechanism locally actuated with an act-and-wait controller. *Mechanism and Machine Theory*, 159:104253, 2021. doi: 10.1016/j.mechmachtheory.2021.104253.

[10] A. Antoniou and W-S. Lu. *Practical Optimization. Algorithms and Engineering Applications*. Springer, New York, 2007. doi: 10.1007/978-0-387-71107-2.

[11] S. Wu, J. Akroyd, S. Mosbach, G. Brownbridge, O. Parry, V. Page, W. Yang, and M. Kraft. Efficient simulation and auto-calibration of soot particle processes in Diesel engines. *Applied Energy*, 262:114484, 2020. doi: 10.1016/j.apenergy.2019.114484.

[12] L. Mazouz, S.A. Zidi, A. Hafaifa, S. Hadjeri, and T. Benaissa. Optimal regulators conception for wind turbine PMSG generator using Hooke Jeeves method. *Periodica Polytechnica Electrical Engineering and Computer Science*, 63(3):151–158, 2019. doi: 10.3311/PPee.13548.

[13] L. Benasla, A. Belmadani, and M. Rahli. Hooke-Jeeves' method applied to a new economic dispatch problem formulation. *Journal of Information Science and Engineering*, 24(3):907–917, 2008.

[14] C. Li and A. Rahman. Three-phase induction motor design optimization using the modified Hooke-Jeeves method. *Electric Machines & Power Systems*, 18(1):1–12, 1990. doi: 10.1080/07313569008909446.

[15] L. Litvinas. A hybrid of Bayesian-based global search with Hooke–Jeeves local refinement for multi-objective optimization problems. *Nonlinear Analysis: Modelling and Control*, 27(3):534–555, 2022. doi: 10.15388/namc.2022.27.26558.

[16] T.M. Alkhamis and M.A. Ahmed. A modified Hooke and Jeeves algorithm with likelihood ratio performance extrapolation for simulation optimization. *European Journal of Operational Research*, 174(3):1802–1815, 2006. doi: 10.1016/j.ejor.2005.04.032.

[17] M.F. Tabassum, M. Saeed, N.A. Chaudhry, J. Ali, M. Farman, and S. Akram. Evolutionary simplex adaptive Hooke-Jeeves algorithm for economic load dispatch problem considering valve point loading effects. *Ain Shams Engineering Journal*, 12(1):1001–1015, 2021. doi: 10.1016/j.asej.2020.04.006.

[18] S.C. Chapra and R. Canale. *Numerical Methods for Engineers*. Sixth ed. McGraw-Hill, New York, 2010.

[19] C. Zhang, S. Hu, Y. Liu and Q. Wang. Optimal design of borehole heat exchangers based on hourly load simulation. *Energy*, 116(1):1180–1190, 2016. doi: 10.1016/j.energy.2016. 10.045.

[20] M.H. Heydari, Z. Avazzadeh, C. Cattani. Taylor's series expansion method for nonlinear variable-order fractional 2D optimal control problems. *Alexandria Engineering Journal*, 59(6):4737–4743, 2020. doi: 10.1016/j.aej.2020.08.035.